

Robust Coordinated Longitudinal Control of MAV Based on Energy State

Chenlong Zhang^{1,2}, Dawei Li², and Haodong Li^{1,2}

¹ School of Automation Science and Electrical Engineering, Beihang University, Beijing 100191, China

² Institute of Unmanned System, Beihang University, Beijing 100191, China

Abstract. Fixed-wing Miniature Air Vehicle (MAV) is not only coupled with longitudinal motion, but also more susceptible to wind disturbance due to its lighter weight, which brings more challenges to its altitude and airspeed controller design. Therefore, in this paper, an improved longitudinal control strategy based on energy state, is proposed to address the above-mentioned issues. The control strategy utilizes the Linear Extended State Observer (LESO) to observe the energy states and the disturbance of the MAV, and then designs a Multiple-Input Multiple-Output (MIMO) controller based on a more coordinated Total Energy Control (TEC) strategy to control the airspeed and altitude of the MAV. The performance of this control strategy has been successfully verified in a Model-in-the-Loop (MIL) simulation with Simulink, and a comparative test with the classical TEC algorithm is carried out.

Keywords: Total Energy Control (TEC), Extended State Observer (ESO), Miniature Air Vehicle (MAV), Longitudinal Control

1 Introduction

MAV specifically refers to fixed-wing Unmanned Aerial Vehicles (UAVs) with a wingspan of less than 5 feet[1]. The conventional longitudinal control system of MAV adopts the design method of Single-Input Single-Output (SISO), such as the altitude and the airspeed are controlled by the elevator and the throttle, respectively. However, this approach results in uncoordinated longitudinal control and insufficient flight envelope protection[2].

In order to overcome the inherent shortcomings of the classical SISO controller mentioned above, Lambregts proposed the concept of TEC, which designed a longitudinal controller of MAV from the perspective of controlling the variation and distribution of the total energy of MAV[3]. Then Faleiro et al. analyzed the superiority of the MIMO controller based on TEC, and designed an improved TEC controller using the method of eigenstructure assignment[4]. Based on the research of Faleiro and Lambregts, QZ Zhang et al. introduced deviation control into the TEC controller, and realized the zero steady-state error control of the altitude and airspeed[5,6].

Nowadays, the fixed-wing longitudinal controllers in the famous open source projects Ardupilot³ and PX4⁴ for UAVs are all designed based on TEC. And many researchers also combine TEC with other control strategies to improve controller performance. Ying-Chih Lai et al. accomplished Optimal Energy Control System (OECS) using Linear-Quadratic-Gaussian (LQG) and gain scheduling control[7]. Brigido-González et al. proposed a nonlinear description of TEC, and adopted an adaptive strategy to design the TEC controller[8]. Degaspere et al. proposed a more integrated TEC control framework using robust control theory by adding engine related variables to TEC architecture[9]. Furthermore, Elgohary et al. completed the hardware-in-the-loop(HIL) simulation of the TEC-based altitude hold controller using Simulink[10], and Jimenez et al. completed the real-world test of the TEC controller using a low-cost MAV[11].

However, the focus of the above methods does not consider the effect of turbulence, which is a challenge that can not be ignored for MAVs. Therefore, in this paper, we explore the transformation between the energy states and the control actuators, and improve the basic architecture of TEC in conjunction with Linear Active Disturbance Rejection Control (LADRC) for stronger robustness. And the superiority of the designed control scheme, which is subsequently called LADRC-TEC, is demonstrated by comparison with the classical TEC scheme.

The remainder of this paper is structured as follows. Section 2 briefly describes the principles of TEC and LADRC. Section 3 derives energy state differential equations of the MAV, and details the internal structure of the LADRC-TEC. Section 4 completes the simulation experiments through Simulink. Finally, Section 5 summarizes the work of the full paper and indicates the future work.

2 The Principle of TEC and LADRC

2.1 Longitudinal Motion and Coupling Characteristics of MAV

The longitudinal kinematic equations of the MAV in its body frame[12,13] are:

$$\begin{cases} \dot{h} = u \sin \theta - v \sin \phi \cos \theta - w \cos \phi \cos \theta \\ \dot{u} = rv - qw - g \sin \theta + \frac{A_x^b + T}{m} \\ \dot{w} = qu - pv + g \cos \theta \cos \phi + \frac{A_z^b}{m} \\ \dot{\theta} = q \cos \phi - r \sin \phi \\ \dot{q} = \Gamma_5 pr - \Gamma_6 (p^2 - r^2) + \frac{M_{pitch}}{J_y} \end{cases} \quad (1)$$

where h represents the altitude of the MAV; $[u, v, w]^T$ and $[p, q, r]^T$ are the linear velocities and the angular velocities of the MAV, respectively; A_x^b and A_z^b represent the components of the aerodynamic force under the x-axis and z-axis of the body frame, respectively; T represents the thrust of the propeller; m represents the total weight of the MAV; θ and ϕ represent the pitch angle and the roll angle, respectively.

³ <https://ardupilot.org/>

⁴ <https://px4.io/>

A_x^b and A_z^b are related to the lift L and the drag D as follows:

$$A_x^b = L \sin \alpha - D \cos \alpha, A_z^b = -L \cos \alpha - D \sin \alpha$$

where α represents the angle of attack.

Under the condition of stable level flight without wind, there is $\phi = v = p = r = 0$. Because $\alpha = \tan^{-1}(\frac{w}{u}) \approx 0$, there is $w \approx 0$, at this time the airspeed $V_a = u$.

Then Eq.(1) can be simplified as:

$$\begin{cases} \dot{h} = V_a \sin \theta \\ \dot{V}_a = \frac{T-D}{m} - g \sin \theta \end{cases} \quad (2)$$

It can be seen from Eq.(2) that for the MAV, the change of pitch angle will lead to the change of MAV's altitude and airspeed; the change of thrust will lead to the change of MAV's airspeed, and subsequently lead to the change of MAV's altitude.

Due to these kinematically coupled characteristics of the MAV, SISO-based controllers will lead to inconsistencies in control, resulting in excessive waste of energy and longer response times.

2.2 The Principle of TEC

The TEC decouples the altitude and airspeed control by controlling and distributing the total energy of the MAV. The throttle and the elevator are utilized to control the total energy variation and the total energy distribution of the MAV, respectively.

The total energy of the MAV includes the kinetic energy and gravitational potential energy of the MAV:

$$E_T = E_D + E_S = \frac{1}{2} m V_a^2 + mgh \quad (3)$$

Then, the total energy rate of MAV is:

$$\dot{E}_T = m V_a \dot{V}_a + mg \dot{h} \quad (4)$$

Considering that the pitch angle of MAV is generally relatively small when flying smoothly, we assume $\sin \theta \approx \theta$. Then from Eq.(2), it can be deduced that the required thrust during flight is:

$$T = mg \left(\frac{\dot{V}_a}{g} + \theta \right) + D \quad (5)$$

From Eq.(2), Eq.(4) and Eq.(5), we can get:

$$\dot{E} = \frac{\dot{E}_T}{mg V_a} = \frac{\dot{V}_a}{g} + \theta = \frac{T-D}{mg} \quad (6)$$

where \dot{E} represents the specific energy rate.

Assuming that the drag of the UAV is constant during flight, then the change of thrust of the MAV is only related to the change of pitch angle and airspeed of MAV. Consequently, the following relationship is formulated:

$$\Delta T = mg \left(\frac{\Delta \dot{V}_a}{g} + \Delta \theta \right) \propto \Delta \dot{E} \quad (7)$$

where ΔT represents the change in thrust, $\Delta \dot{V}_a$ represents the change in airspeed, $\Delta \theta$ represents the change in pitch angle, $\Delta \dot{E}$ represents the change in specific energy rate.

From this, we can obtain the control law based on the PI controller, which controls the thrust change by controlling the total energy change of the MAV:

$$T^d = k_{Ep} \Delta \dot{E} + \int_{t_0}^t k_{Ei} \Delta \dot{E} dt + T^* \quad (8)$$

where T^d represents the desired thrust after the flight state changes; T^* is the nominal thrust of the MAV in the cruise phase; k_{Ep} and k_{Ei} represent the proportional and integral gain, respectively.

Analogously, the concept of specific energy distribution rate is introduced for controlling the total energy distribution, which is defined as:

$$\dot{B} = \theta - \frac{\dot{V}_a}{g} \quad (9)$$

Similar to the above control law, the transitive relationship between the desired pitch angle θ^d and the change of specific energy distribution rate $\Delta \dot{B}$ is expressed as follows:

$$\theta^d = k_{Bp} \Delta \dot{B} + \int_{t_0}^t k_{Bi} \Delta \dot{B} dt \quad (10)$$

where θ^d represents the desired pitch angle after the flight state changes; k_{Bp} and k_{Bi} represent the proportional and integral gain, respectively.

In order to avoid introducing unnecessary zeros into the control system, combining Eq.(8) and Eq.(10), the core algorithm of TEC theory can be simplified as [4]:

$$\begin{cases} T^d = k_{Ep} \dot{E} + \int_{t_0}^t k_{Ei} \Delta \dot{E} dt + T^* \\ \theta^d = k_{Bp} \dot{B} + \int_{t_0}^t k_{Bi} \Delta \dot{B} dt \end{cases} \quad (11)$$

2.3 The Principle of LADRC

The LADRC is proposed by ZQ Gao, which mainly includes LESO and linear state error feedback controller (LSEFC)[14]. LESO is utilized to observe the total disturbance of the plant and expand it into a new state variable. LSEFC

adopts the feedforward control strategy to compensate the total disturbance of the plant based on the order of the plant. Its control architecture is shown in Fig.1.

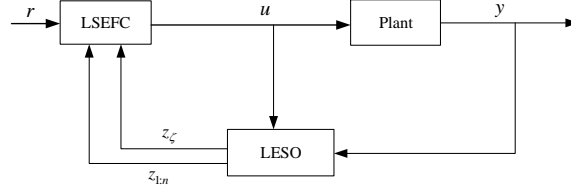


Fig. 1. Architecture of LADRC. $z_{1:n}$ and z_{ζ} represent the original state variables and observed disturbances of the plant, respectively; y and u are the output and input of the plant, respectively; r is the input of the controller.

Next, the structure of LADRC is further elaborated through a second-order system. Let the controlled object be:

$$\ddot{y} = a_1 \dot{y} + a_0 y + d + bu \quad (12)$$

where d is the disturbance.

By setting d to the extended state, which means that the state variable is $\mathbf{x} = [y \ \dot{y} \ d]^T$, Eq.(12) can be converted into a continuous extended state space description:

$$\begin{cases} \dot{\mathbf{x}} = \mathbf{A}\mathbf{x} + \mathbf{B}u + \mathbf{E}\dot{d} \\ y = \mathbf{C}\mathbf{x} \end{cases} \quad (13)$$

$$\text{where } \mathbf{A} = \begin{bmatrix} 0 & 1 & 0 \\ a_0 & a_1 & 1 \\ 0 & 0 & 0 \end{bmatrix}, \mathbf{B} = \begin{bmatrix} 0 \\ b \\ 0 \end{bmatrix}, \mathbf{E} = \begin{bmatrix} 0 \\ 0 \\ 1 \end{bmatrix}, \mathbf{C} = [1 \ 0 \ 0].$$

Let the state variable of the observer be $\hat{\mathbf{x}}$, and the corresponding LESO is:

$$LESO : \begin{cases} \dot{\hat{\mathbf{x}}} = (\mathbf{A} - \mathbf{L}\mathbf{C})\hat{\mathbf{x}} + [\mathbf{B}, \mathbf{L}]\mathbf{u}_c \\ \mathbf{y}_c = \hat{\mathbf{x}} \end{cases} \quad (14)$$

where $\mathbf{u}_c = [u \ y]^T$ is the input variable of LESO, $\mathbf{y}_c = [\hat{y} \ \hat{\dot{y}} \ \hat{d}]^T$ is the output variable of LESO, \mathbf{L} is the observer gain matrix to be designed.

Note that \dot{d} is omitted in Eq.(14), because \dot{d} can be estimated by the correction term.

LSEFC can be regarded as a feedforward based Proportional-Integral (PD) controller, which can be expressed as:

$$LSEFC : \begin{cases} u_0 = k_p (r - \hat{y}) - k_d \hat{\dot{y}} \\ u = (u_0 - \hat{d}) / b \end{cases} \quad (15)$$

3 The Design of MAV's Longitudinal Controller

The longitudinal controller of MAV consists of two parts: the outer loop and the inner loop. In the outer loop, we design the LESO to observe energy states of the MAV and the corresponding disturbance, based on dynamic differential equations of \dot{E} and \dot{B} of the MAV, which reveal the inherent flaws of traditional TEC. And then we utilize a MIMO controller, which has a more coordinated transfer relationship between energy states and control quantities, to calculate the desired pitch angle and thrust. The inner loop is used to pass the desired pitch angle and thrust commands to the elevator and the throttle. The overall control system architecture is shown in Fig.2.

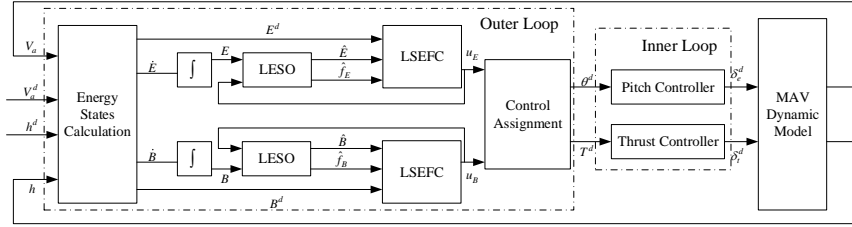


Fig. 2. Architecture of LADRC-TEC. $(\)^d$ represents the desired value. $(\hat{\ })$ represents the estimate of LESO.

3.1 The Design of Inner Loop Controller

The Design of Thrust Controller Usually, MAV is an electric aircraft, and the corresponding thrust is generated by the rotation of the propeller, so a simplified propeller thrust model can be generated by using Bernoulli's principle[15]:

$$T = \frac{1}{2} \rho S_{prop} C_{prop} (k_{motor}^2 \delta_t^2 - V_a^2) = k_{T1} \delta_t^2 - k_{T2} V_a^2 \quad (16)$$

where k_{T1} and k_{T2} are constant parameters related to the propeller motor.

So a feedback-free thrust controller can be expressed as:

$$\delta_t^d = \sqrt{\frac{T^d + k_{T2} V_a^2}{k_{T1}}} \quad (17)$$

The most significant advantage of using this kind of thrust controller is that we can skip the MAV's thrust control command and directly generate the MAV's throttle control command when designing the outer loop controller.

The Design of Pitch Controller To simplify the controller design process, the pitch controller is implemented with a PID controller:

$$\delta_e^d = k_{p,\theta} (\theta^d - \theta) + k_{i,\theta} \int_{t_0}^t (\theta^d - \theta) dt - k_{d,\theta} \dot{\theta} \quad (18)$$

3.2 The Design of Outer Loop Controller

In the condition of stable flight with no wind and no sideslip, there is $V_a = \sqrt{u^2 + w^2}$, so

$$\dot{V}_a = \frac{u\dot{u} + w\dot{w}}{V_a} = \dot{u}\cos\alpha + \dot{w}\sin\alpha \quad (19)$$

Substituting into Eq.(1), we have

$$\begin{aligned} \dot{V}_a &= \cos\alpha \left\{ rv - qw - g \sin\theta + \frac{A_x^b + T}{m} \right\} + \\ &\quad \sin\alpha \left\{ qu - pv + g \cos\theta \cos\phi + \frac{A_z^b}{m} \right\} \\ &= -g \sin(\theta - \alpha) - g \sin\alpha \cos\theta (1 - \cos\phi) + \frac{T \cos\alpha - D}{m} \\ &= -g \sin(\theta - \alpha) + \frac{T - D}{m} + d_V \end{aligned} \quad (20)$$

where $d_V = -g \sin\alpha \cos\theta (1 - \cos\phi) + \frac{T}{m} (\cos\alpha - 1)$ is regarded as the disturbance of the system. In the condition of level straight flight, there is $d_V \approx 0$.

Usually the drag can be expressed as $D = \frac{1}{2} \rho V_a^2 S C_D$, so Eq.(20) can be linearized as:

$$\begin{aligned} \dot{\widetilde{V}}_a &= -g \cos(\theta^* - \alpha^*) \widetilde{\theta} + \frac{2k_{T1}\delta_t^*}{m} \widetilde{\delta}_t + \frac{\rho S C_D V_a^* - 2k_{T2}V_a^*}{m} \widetilde{V}_a \\ &\quad + d_V + R_n \\ &= a_1 \widetilde{\theta} + a_2 \widetilde{\delta}_t + a_3 \widetilde{V}_a + d_V + R_n \end{aligned} \quad (21)$$

where $\widetilde{V}_a = \dot{V}_a - \dot{V}_a^* = \dot{V}_a$, $\widetilde{\theta} = \theta - \theta^*$, $\widetilde{\delta}_t = \delta_t - \delta_t^*$, $\widetilde{V}_a = V_a - V_a^*$; a_1, a_2 and a_3 are constants that can be calculated from the aerodynamic parameters of the MAV; R_n is the remainder of the Taylor polynomial. V_a^*, θ^* and δ_t^* are the nominal values at cruise.

From Eq.(1), we get:

$$\begin{aligned}
\dot{h} &= u \sin \theta - v \sin \phi \cos \theta - w \cos \phi \cos \theta \\
&= V_a \theta + (u \sin \theta - V_a \theta) - v \sin \phi \cos \theta - w \cos \phi \cos \theta \\
&= V_a \theta + d_h
\end{aligned} \tag{22}$$

where d_h is regarded as the disturbance of the system, and $d_h \approx 0$ in the condition of level straight flight.

Therefore

$$\begin{aligned}
\dot{E} &= \frac{\dot{V}_a}{g} + \frac{\dot{h}}{V_a} \\
&= \frac{a_1}{g}(\theta - \theta^*) + \frac{a_2}{g}(\delta_t - \delta_t^*) + \frac{a_3}{g}(V_a - V_a^*) + \frac{d_V + R_n}{g} + \theta + \frac{d_h}{V_a} \\
&= a_{E1}\theta + a_{E2}\delta_t + f_E \\
&= b_E u_E + f_E
\end{aligned} \tag{23}$$

where u_E is the composite input about θ and δ_t , f_E is the total disturbance with respect to \dot{E} including external disturbance and internal disturbance.

For the first-order system represented by Eq.(23), LESO can be designed as:

$$\begin{cases} e_E = E - \hat{E} \\ \dot{\hat{E}} = \hat{f}_E + b_E u_E + L_1 e_E \\ \dot{\hat{f}}_E = L_2 e_E \end{cases} \tag{24}$$

where L_1 and L_2 are the observer gains to be designed.

After E and f_E are both observed by LESO, LSEFC can be designed as:

$$\begin{cases} u_{E0} = k_E(E^d - \hat{E}) \\ u_E = u_{E0} - \frac{\hat{f}_E}{b_E} \end{cases} \tag{25}$$

where k_E and b_E are adjustable controller gains, $E^d = \int_{t_0}^t \left(\frac{\dot{V}_a^d}{g} + \frac{\dot{h}^d}{V_a} \right) dt$ is the expected specific energy.

The desired airspeed change rate \dot{V}_a^d and the desired altitude change rate \dot{h}^d can be calculated by the following equations:

$$\begin{cases} \dot{V}_a^d = k_V(V_a^d - V_a) \\ \dot{h}^d = k_h(h^d - h) \end{cases} \tag{26}$$

where k_V and k_h are gain factors.

Similarly, for the specific energy distribution rate \dot{B} , there is:

$$\begin{aligned}
\dot{B} &= -\frac{\dot{V}_a}{g} + \frac{\dot{h}}{V_a} \\
&= a_{B1}\theta + a_{B2}\delta_t + f_B \\
&= b_B u_B + f_B
\end{aligned} \tag{27}$$

where u_B is the composite input about θ and δ_t , f_B is the total disturbance with respect to \dot{B} including external disturbance and internal disturbance.

The design process of specific energy distribution rate's LESO and LSEFC is similar to that of \dot{E} , and will not be repeated here.

From Eq.(23) and Eq.(27), it can be seen that:

$$\begin{bmatrix} b_E u_E \\ b_B u_B \end{bmatrix} = \begin{bmatrix} a_{E1} & a_{E2} \\ a_{B1} & a_{B2} \end{bmatrix} \begin{bmatrix} \delta_t \\ \theta \end{bmatrix} = \mathbf{A} \begin{bmatrix} \delta_t \\ \theta \end{bmatrix} \quad (28)$$

where \mathbf{A} plays a role similar to the control allocation matrix.

Therefore

$$\begin{bmatrix} \delta_t^d \\ \theta^d \end{bmatrix} = \mathbf{A}^{-1} \begin{bmatrix} b_E u_E \\ b_B u_B \end{bmatrix} \quad (29)$$

which means that there is no one-to-one correspondence between \dot{E} , \dot{B} and δ_t^d , θ^d .

In other words, the total energy variation and distribution of the MAV can not be simply controlled by the throttle and the pitch angle, respectively, which is also the defect of the traditional TEC theory. Using the control allocation scheme shown in Eq.(29) will obtain a more coordinated control effect, which will allow the MAV to save more control energy and achieve faster response.

4 Simulation Verification and Result Analysis

Through MIL simulation in Simulink, LADRC-TEC will be verified by comparison with the classical total energy control strategy expressed by Eq.(11), which is subsequently referred to as simply TEC. The purpose of the simulation experiment is to verify the performance of the designed controller from multiple perspectives, including dynamic response, wind resistance and energy consumption. The simulation will build a six-degree-of-freedom nonlinear full-scale equation of the MAV in Simulink, and the lateral controller will be implemented using a simple PD controller. The aerodynamic parameters of the MAV used are from [1], which is the Aerosonde UAV's.

And using the aerodynamic parameters of the Aerosonde UAV, we can calculate $\mathbf{A} = \begin{bmatrix} 5.7639 & -0.0003 \\ -5.7639 & 2.0003 \end{bmatrix}$ in Eq.(28). This indicates that for the Aerosonde UAV, \dot{E} is basically affected by throttle, while \dot{B} is affected by both throttle and pitch angle.

4.1 Simulation Analysis of Step Response

We assume that the airspeed of the MAV is 35m/s, and the altitude of the MAV is 100m during cruise. The altitude step response is to receive the command to climb 10m, and the dynamic response of the MAV is demonstrated in Fig.3a. The airspeed step response is to receive the command to accelerate 5m/s, and

the dynamic response of the MAV is demonstrated in Fig.3b. It can be seen that whether it is altitude response or airspeed response, the settling time of LADRC-TEC is shorter than that of TEC, and the overshoot of LADRC-TEC is also smaller than that of TEC, which reflects that LADRC-TEC has a more coordinated control effect.

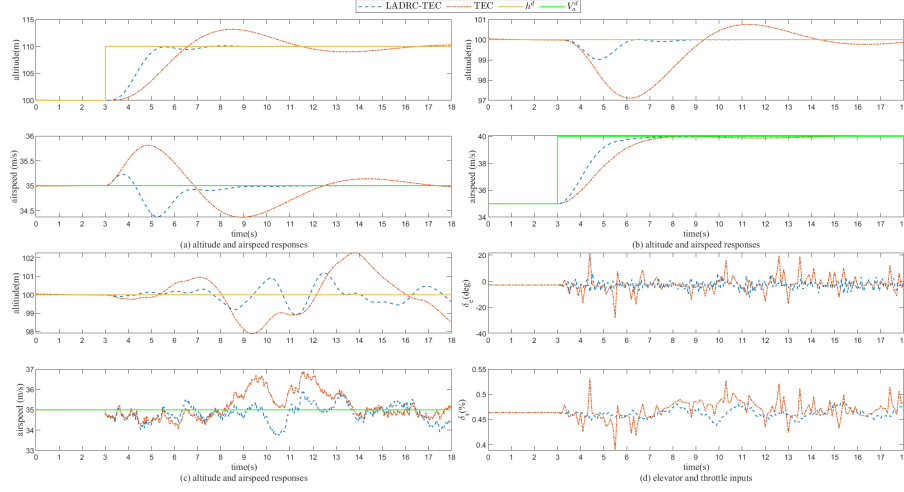


Fig. 3. The dynamic response of MAV

4.2 Simulation Analysis of Wind Disturbance Response

A good model of the turbulent wind field can be obtained by passing the white noise through the shaping filter given by the von Karmen turbulence spectrum. The Dryden transfer function gives an approximation of the von Karmen longitudinal turbulence model as follows[16]:

$$\begin{cases} G_u(s) = \sigma_u \sqrt{\frac{2V_a}{L_u}} \frac{1}{s + \frac{V_a}{L_u}} \\ G_w(s) = \sigma_w \sqrt{\frac{3V_a}{L_w}} \frac{\left(s + \frac{V_a}{\sqrt{3}L_w}\right)}{\left(s + \frac{V_a}{L_w}\right)^2} \end{cases} \quad (30)$$

where σ_u and σ_w represent the turbulence intensity along the x-axis and z-axis of the body frame, respectively; and L_u and L_w are the turbulence scales. These parameters are used to describe different turbulence intensities at different altitudes.

To simulate mild turbulence at low altitudes, the above parameters were chosen as $\sigma_u = 1.06$, $\sigma_w = 0.7$, $L_u = 200$, $L_w = 50$. The generated longitudinal turbulent wind field is demonstrated in Fig.4, which indicates that the maximum velocity of turbulent wind does not exceed 2m/s.

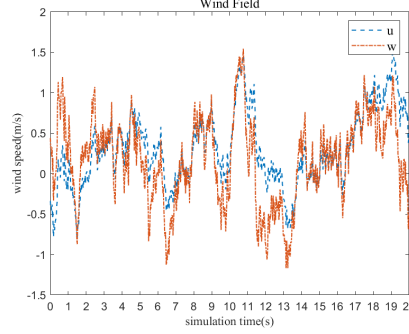


Fig. 4. The Velocity of turbulent wind

In order to evaluate the anti-wind disturbance capability of LADRC-TEC, we set the MAV to cruise steadily in the simulation environment, but suddenly encountered atmospheric turbulence in the 3rd second. The altitude and airspeed responses of the MAV are demonstrated in Fig.3c. The elevator and throttle inputs of the MAV are demonstrated in Fig.3d. Obviously, the altitude and airspeed oscillations and the changes of the control inputs of the MAV using LADRC-TEC strategy are much smaller than those of the MAV using TEC strategy.

If the quantitative analysis method is used, the standard deviation of the MAV's altitude, airspeed, elevator input and throttle input under the nominal cruise condition is calculated. And the results are shown in Table 1, which further validates that LADRC-TEC is more robust.

Table 1. standard deviation of wind disturbance response

	$h(m)$	$V_a(m/s)$	$\delta_e(deg)$	$\delta_t(\%)$
LADRC-TEC	0.4651	0.4524	2.6153	0.0088
TEC	1.0833	0.6733	12.4518	0.1208

5 Conclusion

In this paper, we derived dynamic differential equations of energy states in TEC theory, which show that the coupled control relationship between the en-

ergy states and the longitudinal control actuators. Then based on LESO, we further observed the energy states of the MAV and the corresponding disturbances, which are converted into the desired pitch angle and throttle through the MIMO controller. Through Simulink simulation, we demonstrated that this control strategy has better performance compared with the original TEC control strategy.

However, the performance of the designed controller has only been subjected to preliminary simulation verification, and its feasibility has not been verified in engineering practice.

References

1. Beard, Randal W., Timothy W. McLain: Small unmanned aircraft. Princeton university press (2012).
2. Yayla, M., Kutay, A. T., Kutlu, A.: Energy-based adaptive flight controller for improved coordinated longitudinal control. In: AIAA Scitech 2021 Forum (2021).
3. Lambregts, A.: Vertical flight path and speed control autopilot design using total energy principles. In: Guidance and Control Conference (1983).
4. Faleiro LF, Lambregts AA.: Analysis and tuning of a ‘Total Energy Control System’ control law using eigenstructure assignment. *Aerospace Science and Technology* 3(3), 127–140 (1999).
5. QZ Zhang, JW An, XG Liu: Research on flight track/speed decoupling control method based on aircraft total energy control system (TECS). *Journal of North-western Polytechnical University* 22(3), 384-387 (2004).
6. QZ Zhang, JW An: A new design method of decoupling control system based on aircraft total energy to control flight speed/track. *Acta Aeronautica Sinica* 20025(4), 389-392 (2004).
7. Lai YC, and WO Ting: Design and implementation of an optimal energy control system for fixed-wing unmanned aerial vehicles. *Applied Sciences* 6(11), 369 (2016).
8. Brigido-González JD, Rodríguez-Cortés H: Experimental validation of an adaptive total energy control system strategy for the longitudinal dynamics of a fixed-wing aircraft. *Journal of Aerospace Engineering* 29(1), 04015024 (2016).
9. Giusti Degaspere, Thiago, Karl Kienitz: More Integrated Total Energy Control Law for Longitudinal Automatic Flight Control System Design. In: AIAA Scitech 2020 Forum (2020).
10. Elgohary, A. A., Ashry, A. M., Kaoud, A. M., Gomaa, M. M., Darwish, M. H., Taha, H. E.: Hardware-in-the-loop simulation of UAV Altitude Hold Autopilot. In: AIAA Scitech 2022 Forum (2022).
11. Jimenez, P., Lichota, P., Agudelo and D., Rogowski, K.: Experimental validation of total energy control system for UAVs. *Energies* 13(1), 14 (2019).
12. ML Zhang: Flight control system. Aviation Industry Press, Beijing (1994).
13. ST Wu: Flight Control System. 2nd ed. Beijing University of Aeronautics and Astronautics Press, Beijing (2013).
14. ZQ Gao: Scaling and bandwidth-parameterization based controller tuning. In: Proceedings of the American Conference, pp. 4989-4996 (2003).
15. Argyle M E: Modeling and Control of a Tailsitter with a Ducted Fan. Brigham Young University (2016).
16. Beal, T. R.: Digital simulation of atmospheric turbulence for Dryden and von Karman models. *Journal of Guidance, Control, and Dynamics* 16(1), 132-138 (1993).